Review of Geostationary Interferometric Infrared Sounder

Jianwen Hua (华建文)[1], Zhanhu Wang (王战虎)[1], Juan Duan (段 娟)[1], Libing Li (李利兵)[1], Chenjun Zhang (张晨珺)[1], Xiaowei Wu (吴晓唯)[1,*], Qing Fan (樊 庆)[1], Ren Chen (陈 仁)[1], Xiaojie Sun (孙晓杰)[1], Lianwei Zhao (赵莲维)[1], Qian Guo (郭 倩)[1], Lei Ding (丁 雷)[2], Liwei Sun (孙丽葳)[3], Changpei Han (韩昌佩)[3], Xiangyang Li (李向阳)[4], Nili Wang (王妮丽)[4], Haimei Gong (龚海梅)[4], Xiaoning Hu (胡晓宁)[5], Qingjun Liao (廖清君)[5], Dingquan Liu (刘定权)[6], Tianyan Yu (于天燕)[6], Yinong Wu (吴亦农)[7], Enguang Liu (刘恩光)[7], and Zhijiang Zeng (曾智江)[8]

[1]*Center of Interferometer R&D, Shanghai Institute of Technical Physics, Chinese Academy of Sciences, Shanghai 200082, China*

[2]*Key Laboratory of Infrared System Detection and Imaging Technology, Chinese Academy of Sciences, Shanghai 200082, China*

[3]*Third Engineering Department, Shanghai Institute of Technical Physics, Chinese Academy of Sciences, Shanghai 200082, China*

[4]*Infrared Imaging Material and Device Laboratory, Chinese Academy of Sciences, Shanghai 200082, China*

[5]*Key Laboratory of Infrared Imaging Materials and Detectors, Chinese Academy of Sciences, Shanghai 200082, China*

[6]*Department of Optical Coatings and Materials, Shanghai Institute of Technical Physics, Chinese Academy of Sciences, Shanghai 200082, China*

[7]*Space Cryocooler System Laboratory, Shanghai Institute of Technical Physics, Chinese Academy of Sciences, Shanghai 200082, China*

[8]*State Key Laboratory of Transducer Technology, Chinese Academy of Sciences, Shanghai 200082, China*

**Corresponding author: wuxiaowei@mail.sitp.ac.cn*

Received July 4, 2018; accepted September 29, 2018; posted online November 1, 2018

To measure the global atmospheric three-dimensional distribution and change of temperature and humidity is one of the key areas in atmospheric remote sensing detection; it is also a new research and development direction in the field of meteorological satellite application. As a main element of China second generation of geostationary meteorological satellite Fengyun 4 (FY-4), which was launched on Dec. 11, 2016, the Geostationary Interferometric Infrared Sounder (GIIRS) is the first interferometric infrared sounder working on geostationary orbit internationally. It is used for vertical atmospheric sounding and gains atmospheric temperature, humidity, and disturbances. The combination of Fourier transform spectrometer technology and infrared detectors makes GIIRS have high spectral resolution and large coverage over spatial areas. With this kind of instrument, meteorological satellites can improve the capabilities for severe weather event monitoring and numerical weather prediction. Here a concise review of the GIIRS development project, including its history, missions and functions, technical design, key technologies, system integration, calibration and in-orbit operation status, etc., is presented.

OCIS codes: 120.3180, 120.4820, 120.6200, 300.6300, 300.6340.
doi: 10.3788/COL201816.111203.

The Geostationary Interferometric Infrared Sounder (GIIRS) on the Fengyun 4 (FY-4) meteorological satellite is the first interferometric infrared (IR) sounder working on the geostationary orbit internationally. On September 25, 2017, China Administration of Science, Technology and Industry for National Defense (COSTIND) and China Meteorological Administration held a cooperative news release meeting and declared that the FY-4 meteorological satellite was formally delivered to the user.

The published information gathered by the author demonstrates the earliest mention of the demand on an interferometric IR sounder: the first identification of the need for a geostationary interferometric IR sounder to monitor severe weather was published in the early 1980s by researchers at the University of Wisconsin–Madison, who also developed the High-resolution Interferometric Sounder (HIS) aircraft instrument that demonstrated many of the principles needed to realize the instrument performance[1–6]. Early designs used very small detector arrays, and it was not until the mid-1990s that interferometer designs with large imaging detector arrays were considered. In 1995, China Meteorological Administration held the first symposium on the next generation geostationary meteorological satellite of China, where specialists put forward the conception of the FY-4 meteorological satellite, and GIIRS is one of the main instruments onboard the satellite. In 2000, the function requirements were written in a report at the second symposium on the requirements of the FY-4

meteorological satellite[7]. Then, in 2001, Shanghai Institute of Technical Physics, Chinese Academy of Sciences (SITP) started to invite competent persons; they teamed up to formally work on the pre-research project of GIIRS. At the same time, two projects for exploring this type of technology were under way as well: Geostationary Imaging Fourier Transform Spectrometer (GIFTS)[8] and Meteosat of Third Generation Sounder (MTG-S). GIFTS was a New Millennium Program (NMP) sponsoring instruments designed to validate the technologies of imaging Fourier transform spectroscopy. In 2006, the NASA GIFTS project was completed after 7 years, having successfully demonstrated an engineering model that meets all performance requirements for an imaging high spectral resolution sounder using a 128×128 array for rapid spatial coverage with 4 km sampling. At about the same time, the National Oceanic and Atmospheric Administration (NOAA) conducted design studies of the Hyper-spectral Environment Suite (HES), which would meet similar specifications for the GOES-R satellite of the Geostationary Operational Environmental Satellite (GOES) series[9], but this plan was cancelled in the end because of funding limitations[10]. In Europe, the Meteosat Third Generation IR Sounder (MTG-IRS) is being developed with similar capabilities to GIFTS and is expected to launch in 2023.

The pre-research project of GIIRS was approved formally by the commission on COSTIND in 2004. Actually, this sounder is an imaging Fourier transform spectrometer in space. It is based on an interferometer system. The technologies of the interferometer had a breakthrough in October 2005, and then a prototype was established at the end of 2006; this instrument validated the feasibility of an imaging Fourier transform spectrometer. In the next two years, COSTIND funded further research on the technologies of the FY-4 satellite once more; the funding helped the team to solve the engineering technology problems of interferometer, infrared detector, and opposed piston cryocooler. The pre-research project was completed formally in 2008. Then, it underwent a 2-year engineering demonstration, and, in March 2010, GIIRS was confirmed to fly on the FY-4 satellite. Finally, the satellite was launched on December 11, 2016. From the beginning to the end, the development process of the instrument took almost 15 years.

GIIRS is used for vertical atmospheric sounding, where its primary objective is to measure the global atmospheric three-dimensional distribution and change of temperature and humidity. The instrument can take measurements of atmospheric structure by high frequency, where, on this account, if taking time dimension into consideration, it is a four-dimensional detection in reality. It is appropriate for the large-scale rapid detection that is required for meteorology. The vertical detection, measuring the distribution of temperature and humidity along the height direction, is different with the imager, because the imager is a two-dimensional imaging instrument. In 2004, China Meteorological Administration unambiguously defined the missions of GIIRS as follows.

1) To improve the frequency and the spatial resolution of sounding in support of special weather forecasts (including disastrous weather and aviation weather).
2) To improve precision and vertical resolution of measuring temperature profiles and humidity profiles in support of numerical weather prediction.
3) To implement the observation of greenhouse gases and trace gases in support of researches on atmospheric chemistry and global climate change.

The basic functions of GIIRS are as follows.

1) To measure the radiation of two infrared spectrum bands from earth with high spectral resolution.
2) To measure different regions of earth by a rotating scanning mirror.
3) To perform on-board calibration and radiation calibration.
4) To implement star tracking for the sake of high pointing accuracy of the scanning system.

Figure 1 indicates the technical design of GIIRS. In principle, it is an imaging Fourier transform spectrometer in space. It consists of an interferometer, imaging system, scanning system, detectors, cooling system, calibration system, electronic system, mechanical structure, etc. The IR radiation from earth is reflected by a scanning mirror to the telescope, which compresses the diameter of beams, and then reaches the collimator, where the beams change into parallel rays. Afterwards, these rays are incident on the beam splitter. About 50% of the light is reflected from the surface, and the other 50% is transmitted through. The reflected light and the transmitted light hit a fixed mirror and a moving mirror, respectively, and are reflected back towards the beam splitter. These two beams are split into two parts again; therefore, half of the beams will go back to earth, and the others will be reflected to a dichroic filter. Owing to the movement of the moving mirror, the total optical path difference (OPD) between the two beams changes constantly. On the dichroic filter, the beams split to a long-wavelength band and a mid-wavelength band, where the spectral range is 700–1130 cm^{-1} (8.85–14.3 μm) and 1650–2250 cm^{-1} (4.44–6.06 μm). After passing through the aft optics assembly, these IR rays finally reach the detectors.

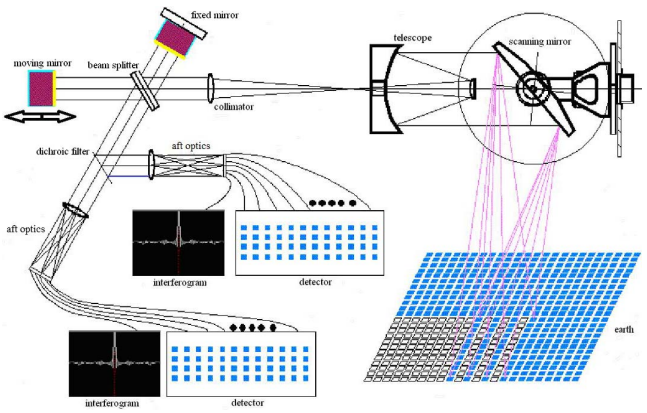

Fig. 1. Technical design on GIIRS of the FY-4 satellite.

The whole optics system is an imaging optics system, and the detectors and earth conjugate with each other. The detector of each wave band has 32×4 sensor elements. GIIRS can implement the observation of different regions by a rotating scanning mirror. When the scanning mirror is pointing to the object, the light intensity of each detector changes with the motion of the moving mirror. With the use of the IR signal data acquisition system, the modulated light intensity is transformed into a digital interferogram.

The cooling system consists of a Stirling cryocooler and a radiant cooler. The Stirling cryocooler can provide the detectors with low temperature working conditions of 65 K, and the radiant cooler can provide working conditions of 200 K for the aft optics assembly. The calibration system includes spectrum calibration and radiation calibration, and its function is to analyze the spectrum and radiation in quantity.

In theory, if two beams are from a common source but traveling over two different paths to a detector, the light intensity at the detector will be determined by

$$I(x) = \int_{\sigma 1}^{\sigma 2} t(\sigma) b(\sigma) \cos(2\pi\sigma x) \mathrm{d}\sigma, \tag{1}$$

where $x = x_2 - x_1$ denotes the OPD, $t(\sigma)$ is the system response factor, σ is the wave number, and $b(\sigma)$ is the spectral amplitude. If the moving mirror moves from one side to another side, the OPD x is over $-X$ to X, and after calibration, the Fourier transform of $I(x)$ is the intensity of the spectrum by the system response factor:

$$\begin{aligned} B(\sigma) &= \mathrm{FT}\{I(x)\} * \mathrm{FT}\{\mathrm{rect}(x)\} \\ &= X \cdot [t(\sigma) b(\sigma)] * \sin c(2\pi X \sigma), \end{aligned} \tag{2}$$

where $\mathrm{FT}\{\bullet\}$ is the Fourier transform operator, $\mathrm{rect}(x)$ is the rectangular window function, and $*$ is the convolution operator.

Characteristics of the design on GIIRS of FY-4 are as follows.

1) To implement the detection of high spectral resolution by using the technologies of a Fourier transform spectrometer with a flat moving mirror interferometer.
2) To conjugate earth with the detectors by using the principle of imaging and an IR sensors array and implement large area detection coverage. Although the array size of the detector is 32×4 at present, the design of GIIRS's field of view and aperture can meet the requirement of 128×128 focal plane arrays (FPAs), and the optical–mechanical system does not need to change a lot when using a large size detector in the future.
3) To cool IR detectors by using two opposed pistons, the cryocooler provides low temperature condition for detectors, and vibration is greatly reduced.
4) To cool the aft optics path by using a radiant cooler decreases IR background.

The working mode of GIIRS is alterable by satellite instruction sent by a ground control system. Some typical modes are defined in Table 1.

The interferometer is the core of GIIRS. Its moving mirror and fixed mirror are both plane reflectors with the advantages of high optical efficiency, light weight, and small size. The material of the beam splitter is zinc selenide. The band of coating is 4.44 to 14.3 μm. The IR light path and reference laser path in the interferometer are designed to share a common optical path, ensuring that they have same OPD. The function of laser interference is to measure OPD accurately. OPD and IR interferogram amplitude

Table 1. Typical Working Mode

Working mode	Performance criterion
Full-disk view of earth	To finish a full-disk view of earth by using the scanning system. View angle coverage is 19°EW × 19°NS
Regional sounding	To observe a specific area by using a designed progressive scan
Sunlight-avoidance sounding	Sunlight may impact the calibration accuracy and the imaging quality of the instrument during eclipse periods. To finish the observation of a given area on the basis of a specific detection mode to avoid these effects
Star tracking	To observe fixed stars by rotating the scanning mirror, the coverage angle is 22.2°, and the brightness is not less than 6.5
Blackbody view	To observe a blackbody by rotating the scanning mirror for implementation of radiation calibration
Deep space view	To observe deep space in specific time intervals according to the different requirements for determining the infrared background
Spectrum calibration	To observe clear atmosphere when pointing to a specific area according to the instructions for spectrum calibration
Orientation	Rapidly pointing to a given position

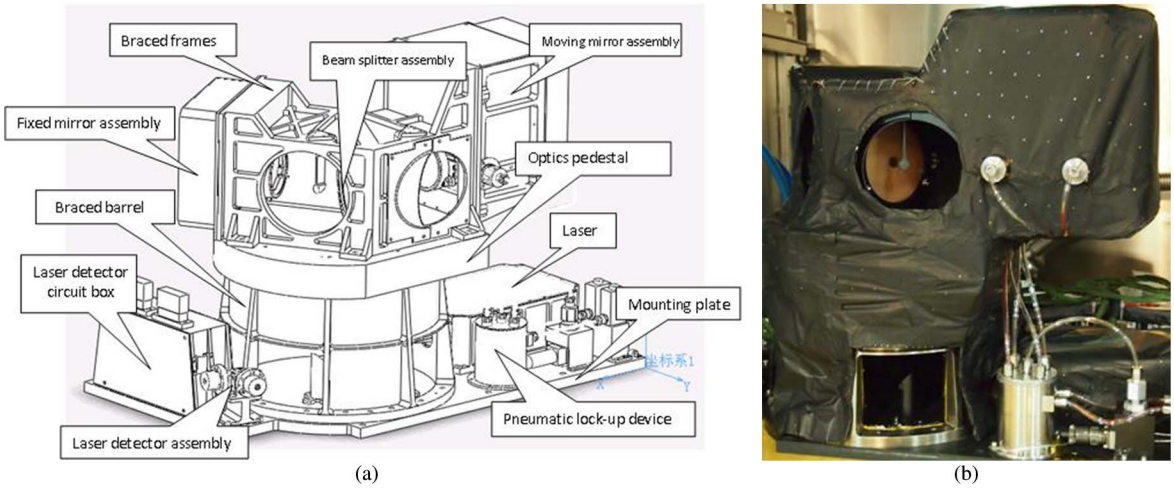

Fig. 2. (a) Mechanical assembly drawing and (b) interferometer product.

are abscissa and ordinate of the interferogram, respectively. Figure 2 shows the photos of the mechanical assembly drawing and interferometer product.

The main functional modules of the mechanical structure are as follows: IR interferometric system, OPD measurement, drive mechanisms of the moving mirror, optical alignment mechanism, frequency stabilized laser, pneumatic locking system, electronic control system, mechanical support structure, etc.

Figure 3 shows the photos of the interferogram obtained by using the interferometer to measure a narrowband light source, where its waveband is 15 cm^{-1}, and center wavelength is 13.8 μm. The bottom part is a magnification of the top in the figure.

Figure 4 shows the photos of the interferogram obtained by the interferometer to measure a hot blackbody.

The research results of the interferometer are as follows.

1) Interferometer: spectral band is 4.44–14.3 μm, maximum OPD is 1.68 cm, aperture is 4 cm, and field of view is 7.9°.

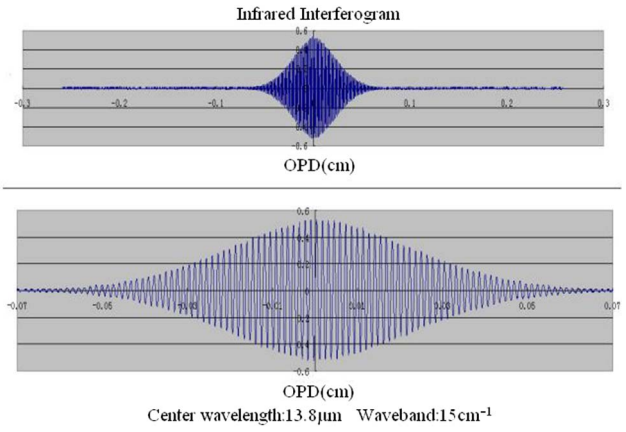

Fig. 3. Interferogram of a narrowband light source.

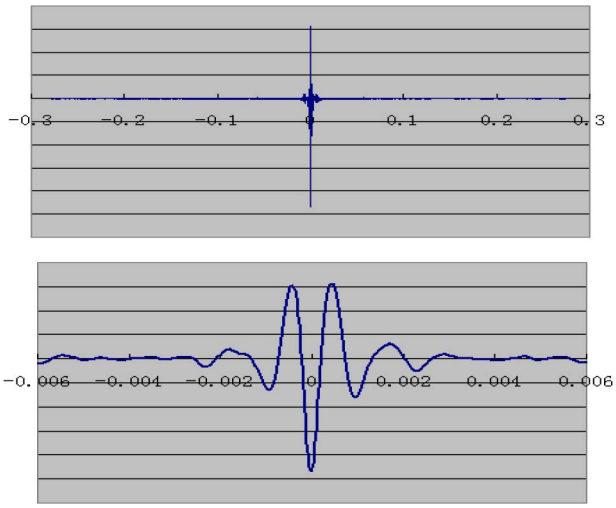

Fig. 4. Interferogram of a hot blackbody.

2) High-precession translation mechanism and plane mirror: its structure has a small size and high optical efficiency.
3) To take space application into consideration, the support structure of the moving mirror is designed with a flexible structure that has no friction, so no lubricant is needed.

This moving mirror Fourier transform spectrometer was developed successfully; this instrument possesses the independent intellectual property and has a wide application in space and also on the ground.

GIIRS is required to cover the 4.44–6.06 μm and 8.85–14.3 μm spectral bands. The former medium-wavelength band adopts an HgCdTe (mercury cadmium telluride, MCT) photovoltaic detector, and the latter long-wavelength band uses an MCT photoconductive detector. Each detector has 32 × 4 sensor elements. Figure 5 shows the photos of the detector assembly. The detectivity of the long-wavelength detector and medium-wavelength

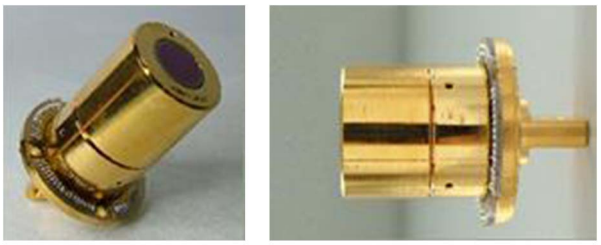

(a) (b)

Fig. 5. Detector assemblies: (a) long-wavelength detector assembly (8.85–14.3 μm) and (b) medium-wavelength detector assembly (4.44–6.06 μm).

detector is 5×10^{10} and 4×10^{11} cm · $Hz^{1/2} \cdot W^{-1}$, respectively.

The cryocooler of GIIRS (Fig. 6) works on the principle of reversed Stirling cycle technology. It is filled with over 10 atm of high-purity helium. The compression piston and displacer piston reciprocate at the frequency of 50 Hz by the driving of the linear motor. The working medium is compressed in the compressor, and released heat dissipates through the heat pipe. Then, the compressed medium transfers to the expander for cooling the detector.

Performance characteristics of the FY-4 cryocooler are tabulated in Table 2.

The function of the radiant cooler is to keep the temperature of the aft optics assembly and interferometer. Figure 7 shows the photo of the radiant cooler.

Performance characteristics of the radiant cooler are tabulated in Table 3.

There are three spectral bands defined for the GIIRS sensor: long wave (8.85–14.3 μm), middle wave (4.44–6.06 μm), and visible light (0.55–0.75 μm).

The optical system includes the following parts:

1) Two-axis scanning mechanism
2) Telescope system
3) Visible light imaging system
4) Interferometric optical system
5) Aft IR cold optical system

Figure 8 shows the structure of the optical system, where the two plane mirrors at the top are scanning mirrors, and the three curved mirrors constitute an off-axis reflective telescope. The first beam splitter is a dichroic splitter, by which visible light is transmitted, and IR light is reflected. Then, visible light goes into the CCD through a set of imaging lenses, where its spatial resolution is 2 km; IR light passes through the interferometer and aft cold optics assembly, finally striking the Dewar detector assembly. The optical aperture of the telescope is 270 mm, the angular view of element is 448 μrad, the telescope's field of view is 1.16°, the compression ratio of the

Fig. 6. Cryocooler of GIIRS.

Table 2. Performance Characteristics of FY-4 Cryocooler

Parameter	Performance
Cooling capability	2 W@60 K (testing environment: 23 ± 5°C)
Input power	≤70 W AC
Vibration force of expander	≤0.7 N(rms)@20–200 Hz
Cooling down time	≤3 h
Mass	≤11 kg
Operating temperature	−25–25°C
Lifetime	Designed for 7 years

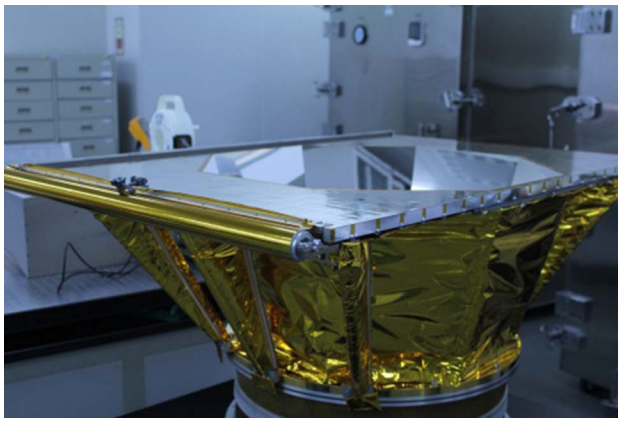

Fig. 7. Radiant cooler.

Table 3. Performance Characteristics of Radiant Cooler

Parameter	Performance
Working temperature of aft optics	195 ± 0.1 K
Performance of radiant cooler	9.4 W@180 K
Heat transfer capability of low temperature heat pipe	10 W@180 K
Temperature difference for heat transfer of low temperature heat pipe	<3 K (testing at 8 W@180 K)

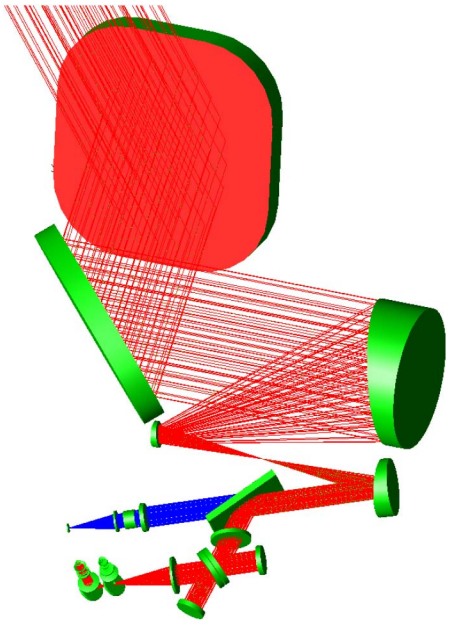

Fig. 8. A conceptual optical system for GIIRS.

beams is 6.75, and the F-number of the optical system is 1. The designed working temperature of the aft optics system and the detection assembly is 200 and 70 K, respectively.

The mechanical structure of GIIRS consists of a main box, baffle, two-axis scanning mechanism, telescope system, interferometer, visible light assembly, aft optics assembly, the support structure of the Dewar detector assembly, the support structure and shield of the cryocooler, blackbody for on-board calibration, temperature controller, etc.

The main box includes a bottom plate, side plate, heat radiation plate, top plate, sling connector, etc. As an important part of GIIRS, it is the main object for temperature control to ensure location change of each optical element within its allowance. On interface, the main box implements the installation with the satellite, the connection between the preamplifier circuit box and the external circuit, the vacuum conversion of Dewar, the locking of the moving mirror, etc. The configuration of the main box is sketched in Fig. 9.

The electronic system consists of eleven circuit modules; their functions are tabulated in Table 4.

According to the desired application, five central processing units (CPUs) and six field programmable gate arrays (FPGAs) are configured. Figure 10 illustrates the electronic system, in which the FPGA in the management of instrument modules is a core, and relationships between modules are shown.

GIIRS is a primary instrument onboard FY-4, which is a new generation of Chinese geostationary meteorological satellite. It implements detection for vertical profiles of atmospheric temperature and humidity with large special coverage, high speed, and high precision by using the technology of a Fourier transformer spectrometer.

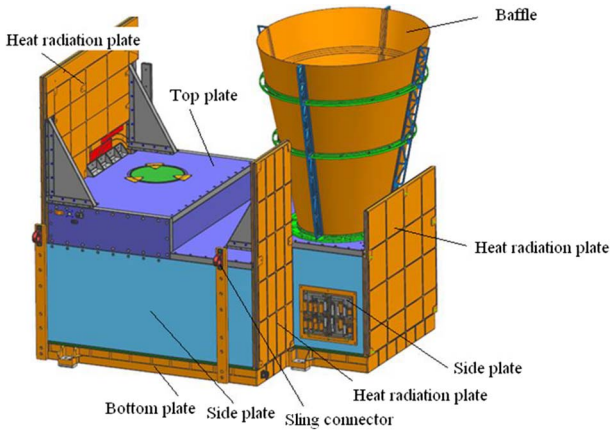

Fig. 9. Configuration of the main box.

The retrieval accuracy of the profiles associates closely with the calibration accuracy. Spectral accuracy and radiometric calibration accuracy from the user's requirement are better than 10^{-5} and less than 1.5 K at 300 K, respectively.

To perform calibration for an IR interferometric hyperspectral instrument, a calibration system is developed (as shown in Fig. 11).

This calibration system can implement the measurements of spectral resolution, instrument line shape (ILS), spectral stability, spectrum calibration, radiation calibration, and detection sensitivity. It consists of a cryogenic off-axis reflective collimator, low temperature blackbody, high-temperature blackbody, mid-IR frequency stabilized laser, long-wave IR frequency stabilized laser, IR wave meter, IR integral sphere, semi-round track structure, IR gas cell, optical platform, calibration docking device, quantitative puff system of high-purity gases, etc. Figure 12 shows a photo of the calibration system at the time of entering the vacuum tank.

(1) Spectral resolution and ILS

Figure 13 shows the measurement records of ILS and the spectral stability of a long-wavelength detector.

In Fig. 13, the top–left part shows the ILS of the long-wavelength detector, the bottom–left part shows the peak-wavelength random change, the top–right part is its statistic bar diagram, and the bottom–right part shows the peak-wavelength distribution obtained from different sensors in one line of the long-wavelength detector.

Figure 14 shows the measurement records of ILS and the spectral stability of the mid-wavelength detector.

In Fig. 14, the top–left part shows the ILS of the mid-wavelength detector, the bottom–left part shows the peak-wavelength random change, the top–right part is its statistic bar diagram, and the bottom–right part shows the peak-wavelength distribution obtained from different sensors in one line of the mid-wavelength detector.

(2) Spectrum calibration

Figure 15 shows the result of spectral calibration for the mid-IR. Figure 16 shows the result of spectral calibration for the long-wave IR.

Table 4. Circuit Modules

Circuit module name	Function description
Data processing and management	Measurement and management of the instrument, information acquisition, and data transmission
GIIRS controller	Control of interferometer electronics and scanning system
Mechanical cryocooler controller	Control of operation for cryocooler
Temperature controller	Measurement and control of temperature in the main box
Chokes	Stabilizing current of cryocooler
Preamplifier circuit of long wave	Amplification of long-wave signal
Preamplifier circuit of mid wave	Amplification of mid-wave signal
Preamplifier circuit of visible light	Amplification of visible light signal
Preamplifier circuit of the inductosyn	Data acquisition and processing for the inductosyn
Laser controller	Control of laser operation
Preamplifier circuit of laser	Amplification of laser signal

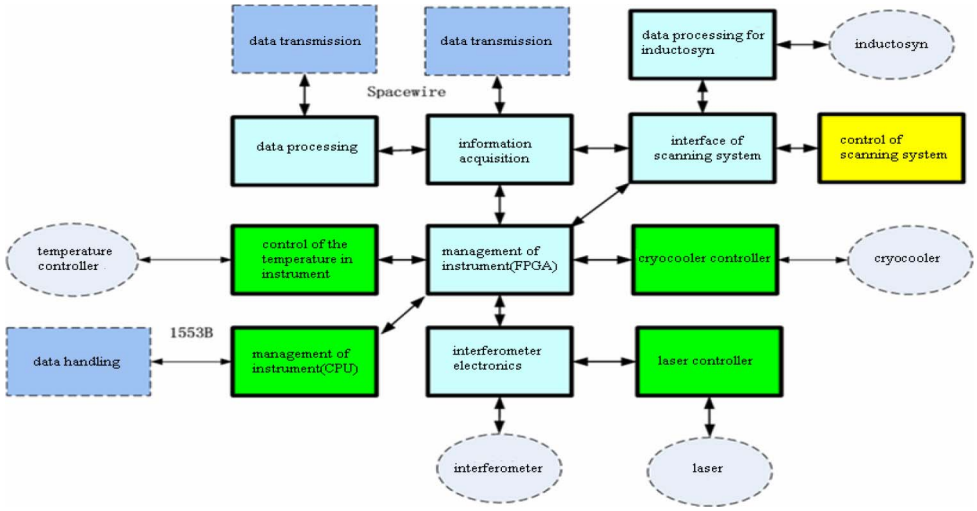

Fig. 10. Electronic system.

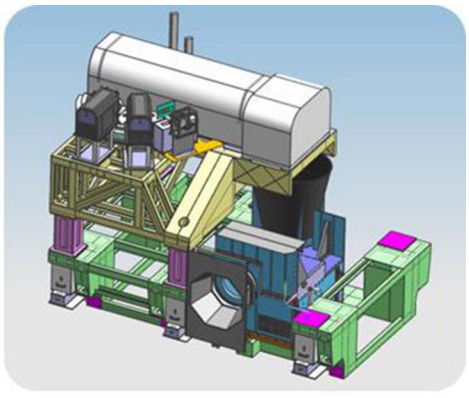

Fig. 11. Calibration system.

Fig. 12. Calibration system entering vacuum tank.

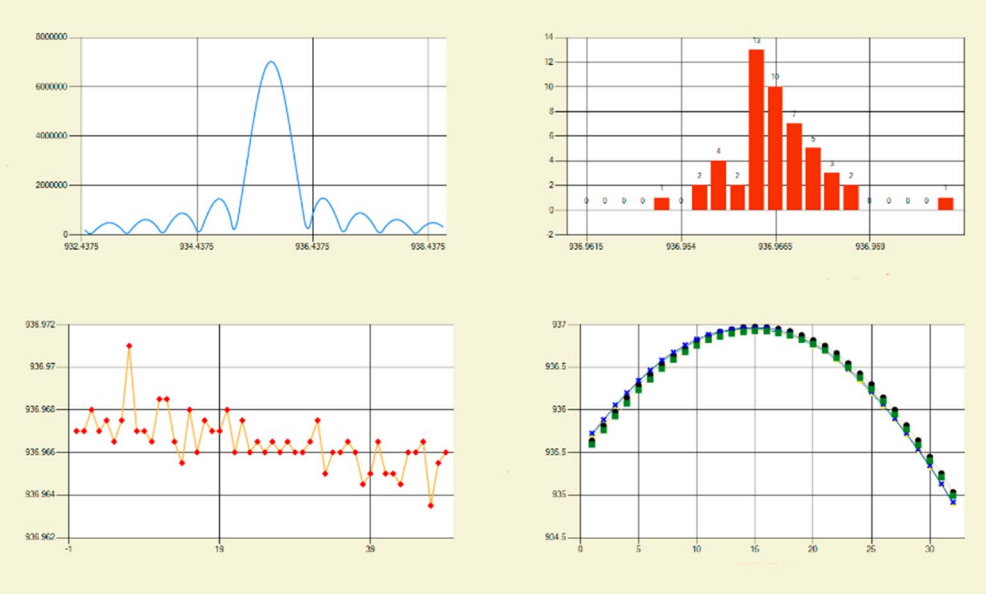

Fig. 13. Instrument line shape (ILS) of long-wavelength detector.

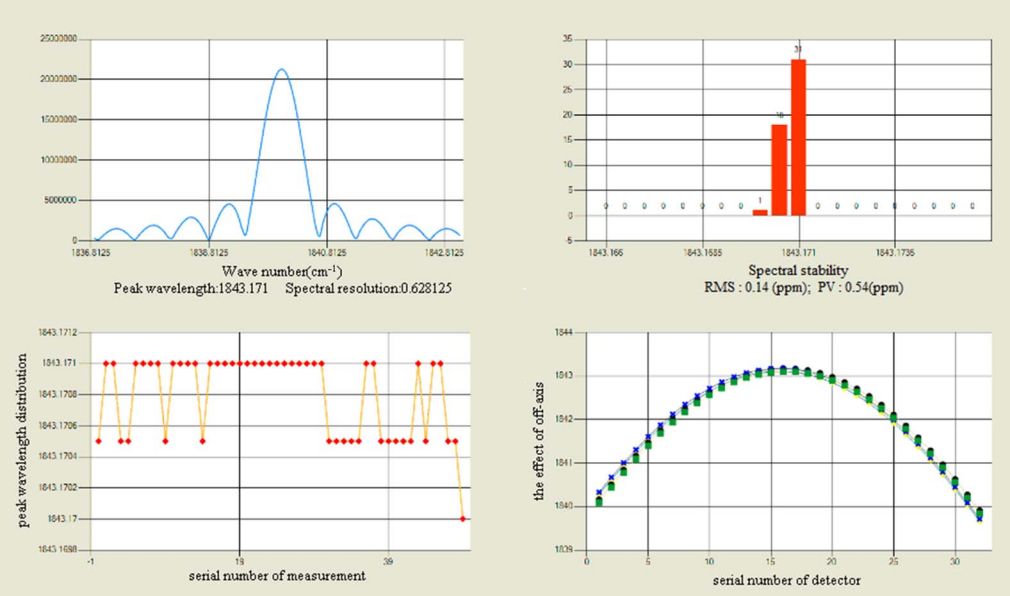

Fig. 14. ILS of mid-wavelength detector.

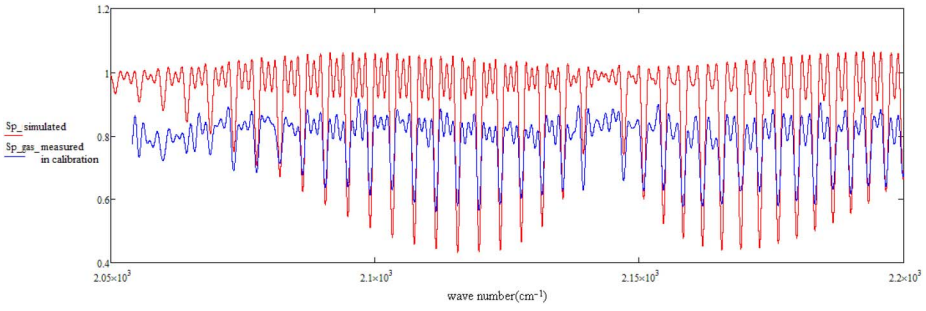

Fig. 15. Mid-wavelength calibration with CO gas.

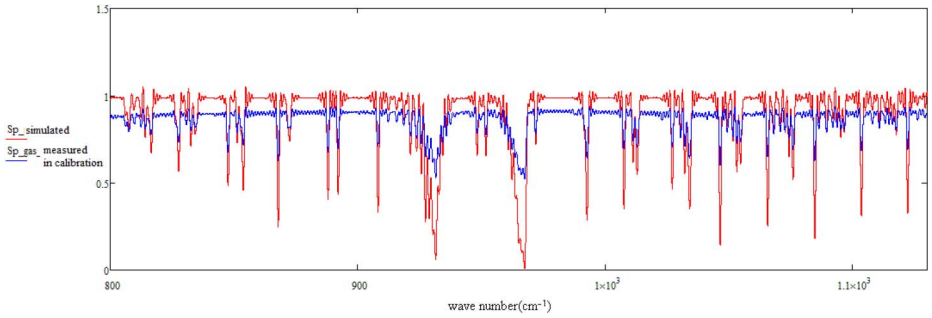

Fig. 16. Long-wavelength calibration with NH_3 gas.

(3) Radiation calibration

(a) The radiation calibration of mid-infrared

The left part of Fig. 17 is the interferograms obtained by pointing a scanning mirror at the blackbody in the mid-wavelength radiation calibration. The right part is all of the interferograms of 128 pixel sensors.

By radiation calibration, the acquired spectral response curve of 128 pixels of the mid-wavelength is shown in Fig. 18.

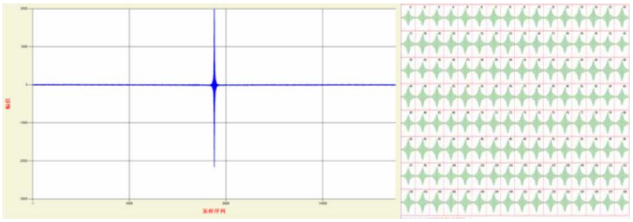

Fig. 17. Interferograms obtained by pointing the scanning mirror at a blackbody.

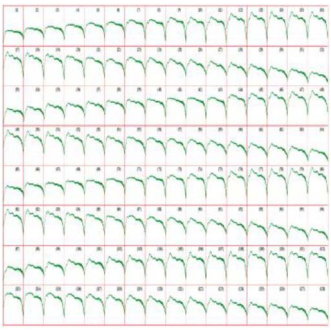

Fig. 18. Spectral response curve of 128 elements.

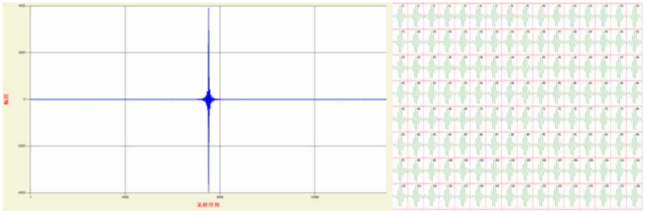

Fig. 19. Interferograms obtained by pointing the scanning mirror at a blackbody.

(b) The radiation calibration of long-IR

The left part of Fig. 19 is the interferograms obtained by pointing a scanning mirror at the blackbody in long-wavelength radiation calibration. The right part is all of the interferograms of 128 pixel sensors.

By radiation calibration, the acquired spectral response curves of 128 elements of the long-wavelength are shown in Fig. 20.

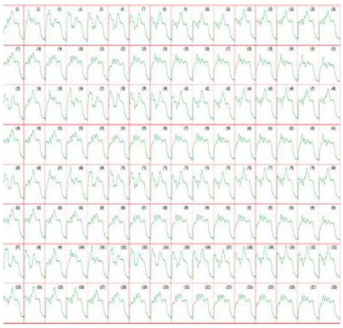

Fig. 20. Spectral response curves of 128 elements.

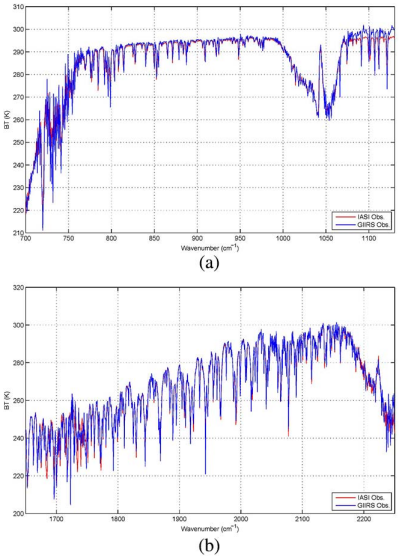

Fig. 21. Atmospheric spectrum sounded in-orbit: (a) long wavelength and (b) mid-wavelength.

After the launch of FY-4 satellite, the following steps are taken to the preparative operation process: temperature control of the instrument, unlocking the moving mirror, decontamination heating of about 45 days, and then the cryocooler starting cooling. The IR detector and interferometer began to work when the temperature reached the designed value. All operation is okay, and every performance of instrument is very good. After a few months, the amplitude of some spectrum bands was reduced. It may be caused by some materials gradually releasing a little gas. Figure 21 shows the photos of the atmospheric spectrum. The blue curve is the air spectrum result sounded by IR Atmospheric Sounding Interferometer (IASI), and the red curve is the air spectrum result sounded by GIIRS.

Table 5. Performance of GIIRS In-orbit

Parameter	Performance
Spectral bandwidth (cm^{-1})	Long wave: 700–1130
	Mid wave: 1650–2250
Spectral resolution (cm^{-1})	0.625
Noise equivalent Radiance [$W/(M^2 \cdot cm^{-1} \cdot rad)$]	Long wave < 0.2
	Mid wave < 0.08
Spatial resolution (km)	16
Time resolution (min)	67 (China)

Since launch, GIIRS has been working properly for nearly one year. Table 5 shows the performance of GIIRS in-orbit.

Figure 22 shows interferograms and spectra obtained by pointing the scanning mirror to different regions on earth.

GIIRS has 1650 equivalent spectral channels to profile the structure of temperature and humidity, just like taking a CT scan for atmosphere. Beside this, GIIRS can take measurement of atmospheric structure continuously with higher frequency compared to sounder on low earth orbit. On this account of time, GIIRS implements a 4-dimensional sounding. It is also the first time to realize this 4-dimensional sounding internationally. As an illustrated example, Fig. 23 is obtained using GIIRS's sounding data.

Scientists want to realize the dream of sounding the temperature and humidity of atmosphere by using the principle of Fourier transform spectral detection for a longtime. Internationally, the history of atmospheric sounding with FTS instruments began in 1969[11] with the launch of the Nimbus meteorological satellite which carried the very successful NASA IRIS instrument (references by Rudy Hanel), which was also widely used in planetary science. This instrument had very large sampling footprints (hundreds of kilometers) and it took decades to achieve the sensitivity needed to reduce footprints to more useful sizes (order of 10 km). Through unremitting efforts, Europe launched polar-orbiting meteorological satellite METOP in 2006, which is equipped with a hyper-spectral IR sounder IASI[12].

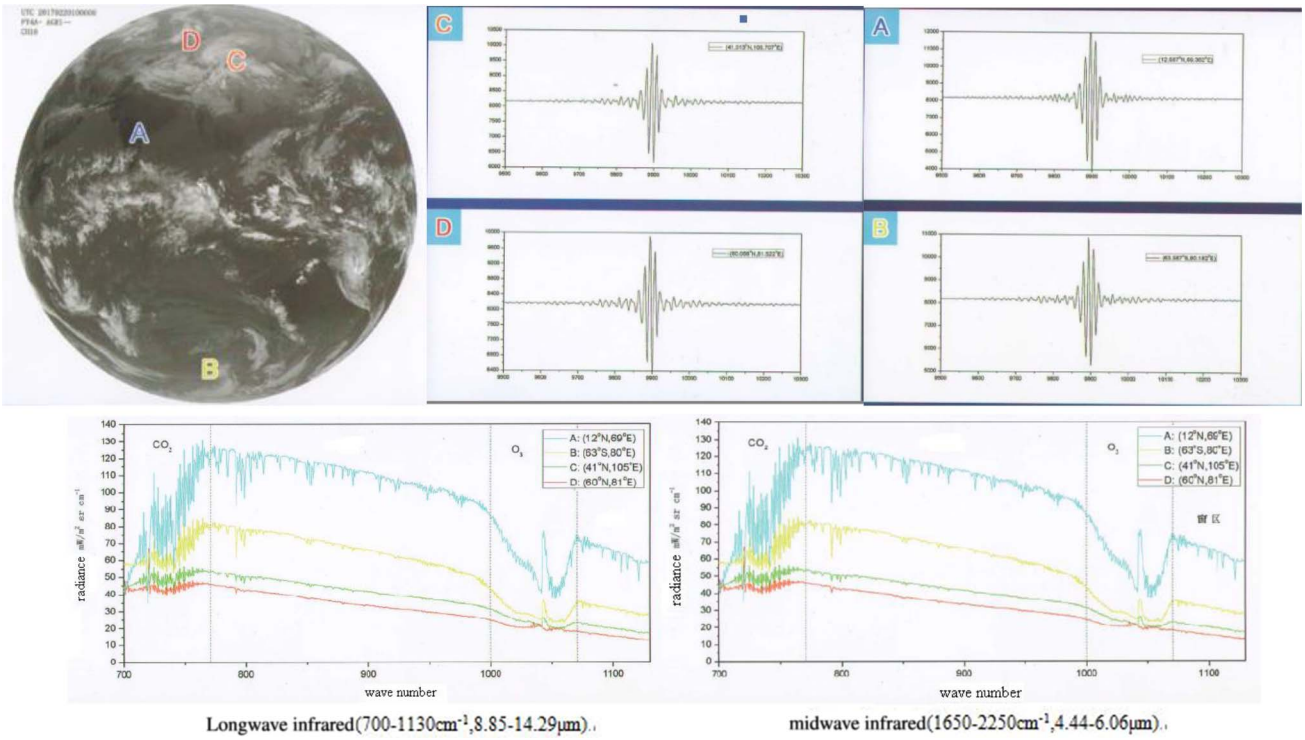

Fig. 22. Interferograms and spectra obtained from different regions: A, India area; B, high latitude of southern hemisphere; C, China area; D, low latitude of northern hemisphere. Sample A indicates relative warm and humid clear atmosphere. Samples B and D represent dry and cold atmospheres. Sample C shows the typical sky.

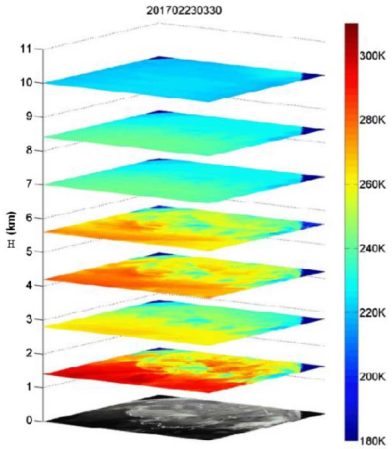

Fig. 23. Vertical distribution of temperature.

Table 6. Main Characteristics of CrIS, IASI, and GIIRS

	Spectral resolution	Detector size	Frequency of observation (approx. times per day)
CrIS	0.625 cm^{-1}	9	4
IASI	0.25 cm^{-1}	4	4
GIIRS	0.625 cm^{-1}	32×4 (=128)	>20 (China area)

In 2011, the Cross-track IR Sounder (CrIS) flew on the National Polar-orbiting Operational Satellite System (NPOESS). These instruments are all Fourier transform IR spectrometers. The GIIRS development program started in 2001 or so and launched in November 2016. After one year of operational testing, Chinese National Satellite Meteorological Center specialists give a high evaluation to it.

Table 6 shows the main characteristics of CrIS, IASI, and GIIRS.

China Meteorological Administration and World Meteorological Organization (WMO) held the Fourth Session of International Strategic Committee (ISCC-4) Meeting on Chinese Meteorological Satellite Programs (November 6–10, 2017 in Hangzhou, China), on which WMO expert and conference chair Tillmann Mohr told reporters that GIIRS, boarded on the FY-4 satellite, allows China to be the world leader of atmospheric sounding on geostationary orbit (http://www.cma.gov.cn/2011xwzx/2011xqxxw/2011xqxyw/201711/t20171108_453476.html?from=timeline).

This work was supported by the China's National Key Special Earth Observation and Navigation Project, Ministry of Science and Technology of China (MOST) (No. 2016YFB0500600). We particularly acknowledge that the high-level GIIRS program specifications were based on the GIFTS specifications.

References

1. W. L. Smith, H. E. Revercomb, H. B. Howell, and H. M. Woolf, in *Fifth Conference on Atmospheric Radiation*, American Meteorological Society (1983).
2. W. L. Smith, H. E. Revercomb, H. B. Howell, and H. M. Woolf, in *International Radiation Symposium '84: Current Problems in Atmospheric Radiation*, G. Fiocco, Ed., Hampton, Virginia (1984), p. 388.
3. W. L. Smith, H. E. Revercomb, H. M. Woolf, H. B. Howell, D. D. LaPorte, and K. Kageyama, in *Proceedings, Symposium on Mesoscale Analysis and Forecasting*, Vancouver, Canada, August 17–19, 1987 (1987), paper ESA SP-282.
4. W. L. Smith, H. E. Revercomb, H. B. Howell, H. M. Woolf, and D. D. LaPorte, *The High Resolution Interferometer Sounder (HIS)* (American Meteorological Society, 1987), p. 271.
5. H. E. Revercomb, H. Buijs, H. B. Howell, D. D. LaPorte, W. L. Smith, and L. A. Sromovsky, Appl. Opt. **27**, 3210 (1988).
6. H. E. Revercomb, D. D. LaPorte, W. L. Smith, H. Buijs, D. G. Murcray, F. J. Murcray, and L. A. Sromovsky, Mikrochimica Acta **95**, 439 (1988).
7. G. Li and F. Zhang, in *The Second Symposium on the Requirements of FY-4 Meteorological Satellite*, National Satellite Meteorological Center (2012), p. 52.
8. W. L. Smith, G. E. Bingham, and H. E. Revercomb, "GIFTS: Revolutionary observations for weather, chemistry, and climate applications," in *Optical Payloads for Space Missions*, S.-E. Qian Ed. (Wiley, 2016).
9. T. J. Schmit, J. Li, S. A. Ackerman, and J. J. Gurka, J. Atmospheric Oceanic Technol. **26**, 2273 (2009).
10. U.S. House of Representatives Committee on Science, Hearing Charter, GAO Report on NOAA's Weather Satellite Program (2006).
11. R. A. Hanel, B. Schlachman, F. D. Clark, C. H. Prokesh, J. B. Taylor, W. M. Wilson, and L. Chaney, Appl. Opt. **9**, 1767 (1970).
12. C. Clerbaux, A. Boynard, L. Clarisse, M. George, J. Hadji-Lazaro, H. Herbin, D. Hurtmans, M. Pommier, A. Razavi, S. Turquety, C. Wespes, and P.-F. Coheur, Atmos. Chem. Phys. **9**, 6041 (2009).